

# <sup>13</sup>C Cross-Polarization and Magic-Angle Spinning Nuclear Magnetic Resonance of Polymorphic Forms of Three Triacylglycerols

T. Arishima<sup>a,\*</sup>, K. Sugimoto<sup>a</sup>, R. Kiwata<sup>a</sup>, H. Mori<sup>a</sup>, and K. Sato<sup>b</sup>

<sup>a</sup>Central Research Institute, Tsukuba R&D Center, Fuji Oil Co. Ltd. Ibaraki, 300-24 Japan and

<sup>b</sup>Faculty of Applied Biological Science, Hiroshima University, Higashi-Hiroshima, 739, Japan

**ABSTRACT:** The cross-polarization and magic-angle spinning nuclear magnetic resonance (CP/MAS-NMR) technique has been used to analyze the polymorphic forms of three triacylglycerols, 1,3-dipalmitoyl-2-oleoyl glycerol (POP), 1, 3-*rac*-palmitoyl-stearoyl-2-oleoyl glycerol (POS), and 1,3-distearoyl-2-oleoyl glycerol (SOS). Specific attention has been paid to glycerol, carbonyl, olefinic, and methyl end carbon resonances. Many distinct differences were observed in each polymorphic form of SOS. In the  $\alpha$  form, the saturated and unsaturated acyl chains exhibit liquid state-like conformations. However, olefinic conformations of the  $\gamma$  and  $\beta'$  forms were asymmetric with respect to the *cis* double bond. Spectral difference between  $\beta_2$  and  $\beta_1$  was observed only for the methylene carbon, and not in the other regions. Spectra of corresponding polymorphic forms of POP and POS were almost identical to those of SOS. However, some spectral differences were observed in the glycerol and methyl regions of  $\gamma$  and  $\beta'$ . From the chemical shifts of the methylene carbons, the crystal structures of the polymorphic form have been discussed, particularly in terms of the subcell structures.

JAOCS 73, 1231–1236 (1996).

**KEY WORDS:** <sup>13</sup>C CP/MAS-NMR, chemical shift, cocoa butter, crystal structure, molecular conformation, polymorphism, solid fat, subcell structure, triacylglycerol.

1,3-Disaturated-2-oleoylglycerols [Sat-O-Sat triacylglycerols (TAG)], such as 1,3-dipalmitoyl-2-oleoylglycerol (POP), 1,3-*rac*-palmitoyl-stearoyl-2-oleoyl glycerol (POS), and 1,3-distearoyl-2-oleoylglycerol (SOS), are major components of confectionery fats (1). Sat-O-Sat TAG usually have several polymorphic forms, and their polymorphic behavior is more complex than that of trisaturated acid triacylglycerols (Sat-Sat-Sat TAG). Sato *et al.* (2–5) studied the polymorphism of these Sat-O-Sat TAG with macroscopic methods and clarified several physical properties, including occurrence, thermodynamic stability, crystal morphology, crystal density, and transformation rate. Recently, Yano *et al.* (6) examined the poly-

morphic structures of POP, POS, and SOS and determined the subcell structure of each polymorphic form, by Fourier-transform infrared absorption (FT-IR), which is a powerful technique for studying the molecular structures of TAG.

Cross-polarization and magic-angle spinning nuclear magnetic resonance (CP/MAS NMR) is also a powerful method for studying molecular conformations (7). CP/MAS NMR spectra give detailed information about the local environment and mobility of specific carbon sites (8). Bociek *et al.* (9) have studied the polymorphic forms of tripalmitin (PPP) and tristearin (SSS) with CP/MAS NMR, and their results are in good agreement with the molecular structures proposed in the literature (10). As for the molecular motion of PPP, Eads *et al.* (11) reported that the most stable form is more restricted than the metastable forms.

In the present study, we used CP/MAS NMR to obtain detailed information about individual sites, such as glycerol, carbonyl, olefinic, and methyl regions in each of the polymorphic form of POP, POS, and SOS. The polymorphic structures obtained are then compared with the results of our previous studies.

## MATERIALS AND METHODS

POP, POS, and SOS samples with a purity of 99.9% were prepared by the following processes. POP, POS, and SOS were initially separated from cocoa butter by solvent-recrystallization from *n*-hexane. Samples with approximately 99% purity were then obtained after preparative high-performance liquid chromatography (HPLC) (Killoprep 250; Millipore Co. Ltd., Milford, MA). The 99.9% samples were then produced with the same HPLC technique from the initial materials of 99% purity. The purity was determined by HPLC (Japan Spectroscopic Co., Tokyo, Japan), which showed no detectable impurity peaks. No analysis of the separation of optical isomers of POS was undertaken.

The occurrence of polymorphs was examined by two modes of crystallization. The first mode involved simple cooling of liquid from 80°C to various crystallization temperatures ( $T_c$ ). The  $\alpha$  forms of POP, POS, and SOS were produced by chilling to 0°C. Other polymorphs of  $\gamma$ ,  $\beta'$ ,  $\beta_2$ , and

\*To whom correspondence should be addressed at Central Research Institute, Tsukuba R&D Center, Fuji Oil Co. Ltd. 4-3 Kinunodai, Yawara, Ibaraki, 300-24 Japan.

$\beta_1$  were obtained by solid-state transformation from the  $\alpha$  form. Identification of independent polymorphs was performed by X-ray diffraction (XRD) (Macscience Cu-K $\alpha$ , Tokyo, Japan) and differential scanning calorimetry (DSC) (Shimadzu, Tokyo, Japan). The two measurements were always taken of the same sample simultaneously by the following procedure: the sample for DSC (1.5–2.0 mg) was separated from the powder sample utilized for XRD (100 mg), and measured at the same time as the XRD scan.

The  $^{13}\text{C}$ -NMR experiments were carried out on a Bruker AC-250 NMR spectrometer (Bruker Instruments Inc., Karlsruhe, Germany), operating at a frequency of 62.83 MHz. A standard Bruker probehead was used for the CP/MAS studies, with a zirconium rotor containing 0.3 g of sample. Spectra were referenced to the residual signal from the carbonyl carbon of glycine at 176.03 ppm relative to a tetramethylsilane (TMS) standard. The experimental conditions used were a single contact pulse of 1 ms and a rotor frequency of 3.5 KHz. Data were collected at a spectral width of 27 KHz, an acquisition time of 74 ms, and a recycle delay of 20 s. Two-hundred scans were accumulated per spectrum, and a line broadening of 5 Hz was used. NMR spectra were measured at  $-10^\circ\text{C}$  to avoid polymorphic transitions. The liquid-state spectra were obtained with a standard high-resolution probehead (5-mm sample tube) at  $23^\circ\text{C}$ .

## RESULTS

We obtained five polymorphic forms of SOS and POP, and three forms of POS. XRD long-spacing and short-spacing of polymorphs of POP, POS, and SOS are summarized in Table 1, and their thermal data from DSC measurements are shown in Table 2.

NMR spectroscopy was used to obtain spectra of both the liquid and crystalline states of the three TAG, POP, POS, and SOS. The chemical shifts of the polymorphic forms and liq-

uid state of the three TAG are summarized in Table 3. The glycerol headgroup regions (50–80 ppm) for the SOS polymorphs are shown in Figure 1, the carbonyl regions (160–180 ppm) in Figure 2, the olefinic regions (120–140 ppm) in Figure 3, and the methyl and methylene regions (10–50 ppm) in Figure 4. The line widths for these solid samples are much broader than those observed in the liquid state. This may result from a distribution of isotropic chemical shifts due to a number of possible noninterchangeable environment for each carbon atom. Many distinct differences in each polymorphic form of SOS were observed as follows.

**Glycerol carbons.** In the glycerol region, two broad peaks at 62.5 and 67.9 ppm were observed with an intensity ratio of 2:1 for the  $\alpha$  form. This is similar to the liquid state, in which the 1- and 3-position of the glycerol are equivalent. The broadness of these peaks results from the different environments of the molecules. In the spectra of the  $\gamma$  form of SOS, two large peaks at 64.7 and 66.6 ppm and a small peak at 59.4 ppm were observed. This indicates that the 1- and 3-position of the glycerol carbons are no longer equivalent. Furthermore, in the  $\beta'$  form, the three glycerol carbon resonances appear as three individual peaks at 60.8, 63.6, and 67.3 ppm, which suggests an asymmetric environment. Two small peaks at 57.6 and 69.0 ppm in the spectrum of the  $\beta'$  form indicate that some  $\beta_2$  crystals are present. The chemical shift of the glycerol carbons at the 1- and 3-position of  $\beta_2$  were observed to have shifted to a higher field than that of the same carbons in other polymorphic forms. However, the chemical shift of the 2-position shifted to lower field. There were no spectral differences between  $\beta_2$  and  $\beta_1$  of SOS.

**Carbonyl carbon.** Spectra of the carbonyl carbons are shown in Figure 2. For the  $\alpha$  form, the physical environment of the three carbonyl carbons in a molecule must be almost identical because they are observed as a single broad peak at 171.4 ppm. The  $\gamma$  and  $\beta'$  forms exhibit a broad and large peak at 172.9 and 173.1 ppm, respectively. The broad peak indi-

**TABLE 1**  
X-Ray Diffraction Long-Spacing and Short-Spacing of Polymorphs of POP, POS, and SOS<sup>a</sup>

	Long-spacing ( $\text{\AA}$ )	Short-spacing ( $\text{\AA}$ ) <sup>b</sup>
POP		
$\alpha$	46.5	4.21(vs)
$\gamma$	65.4	4.74(s) 4.46(m) 3.90(s) 3.58(w)
$\beta'$	42.4	4.38(w) 4.23(s) 4.25(m) 3.96(s) 3.83(w)
$\beta_2$	61.0	4.61(vs) 4.07(m) 3.93(m) 3.82(m) 3.72(m) 3.62(w) 3.55(w) 3.52(w)
$\beta_1$	61.0	4.61(vs) 4.07(m) 3.88(m) 3.82(m) 3.72(m) 3.67(m)
POS		
$\alpha$	47.6	4.23(vs)
$\beta'$	67.9	4.30(w) 4.13(s) 3.85(s)
$\beta$	64.0	4.58(vs) 4.02(w) 3.92(m) 3.85(m) 3.70(s)
SOS		
$\alpha$	48.3	4.21(vs)
$\gamma$	70.5	4.72(s) 4.50(m) 3.88(s) 3.63(w)
$\beta'$	70.0	4.30(m) 4.15(m) 4.02(s) 3.95(m) 3.83(m) 3.70(s)
$\beta_2$	65.0	4.58(vs) 4.00(m) 3.90(m) 3.75(m) 3.67(m) 3.57(w)
$\beta_1$	65.0	4.58(vs) 4.02(w) 3.97(w) 3.85(w) 3.80(w) 3.65(s)

<sup>a</sup>POP, 1,3-dipalmitoyl-2-oleoyl glycerol; POS, 1,3-*rac*-palmitoyl-stearoyl-2-oleoyl glycerol; SOS, 1,3-distearoyl-oleoyl glycerol.

<sup>b</sup>VS: very strong, S: strong, M: medium, W: weak.

**TABLE 2**  
**Thermal Data of POP, POS, and SOS Polymorphs**

	POP		POS		SOS	
	$T_m$ (°C)	$\Delta H_f^a$ (KJ/mol)	$T_m$ (°C)	$\Delta H_f^a$ (KJ/mol)	$T_m$ (°C)	$\Delta H_f^a$ (KJ/mol)
$\alpha$	15.2	68.1 <sup>b</sup>	19.5	41.2 <sup>b</sup>	23.5	47.7 <sup>b</sup>
$\gamma$	27.0	92.5			35.4	98.5
$\beta'$	30.3	95.5	31.6	119.2	36.5	104.8
$\beta_2$	35.1	124.4			41.0	143.0
$\beta_1$	36.7	130.2	35.5	147.8	43.0	151.0

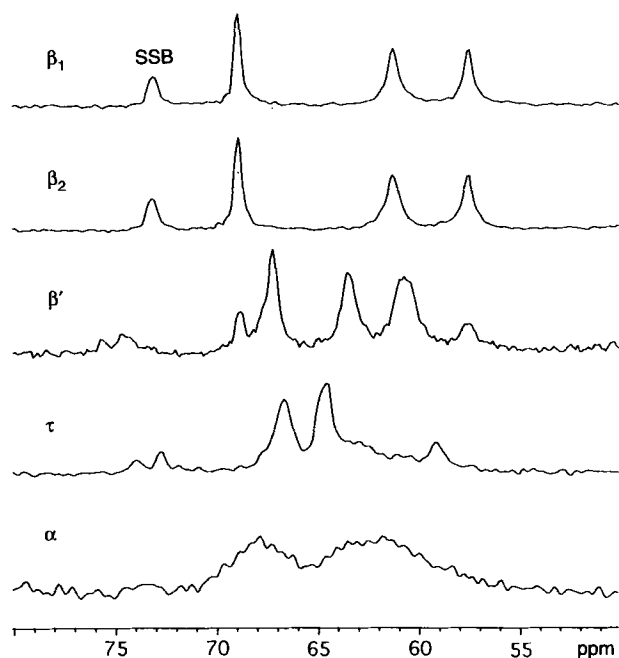
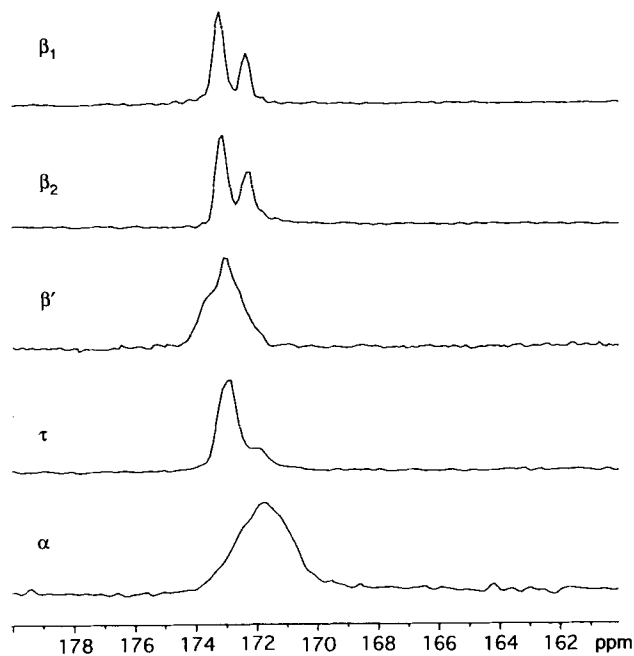
<sup>a</sup>Experimental errors:  $T_m \pm 1^\circ\text{C}$  for  $\alpha$  and  $\pm 0.03^\circ\text{C}$  for others;  $\Delta H_f \pm 7$  KJ/mol for  $\beta_2$  and  $\beta_1$  in POP and SOS,  $\beta$  in POS,  $\pm 3$  KJ/mol for others. See Table 1 for abbreviations.

<sup>b</sup>Enthalpy of melt crystallization was measured on  $\alpha$ .

**TABLE 3**  
 **$^{13}\text{C}$  Chemical Shift of the Liquid and Polymorphic Forms of POP, POS, and SOS<sup>a</sup>**

Group	POP						POS			SOS					
	Liq.	$\alpha$	$\gamma$	$\beta'$	$\beta_2$	$\beta_1$	$\alpha$	$\beta'$	$\beta$	Liq.	$\alpha$	$\gamma$	$\beta'$	$\beta_2$	$\beta_1$
$\text{CH}_2\text{-CH-CH}_2$	62.1	63.6	59.6	63.6	57.8	57.7	62.3	60.9	57.7	62.1	62.5	59.4	60.8	57.6	57.7
$\text{CH}_2\text{-CH-CH}_2$	68.8	68.1	67.3	69.0	69.1	69.1	68.6	68.2	69.1	68.9	67.9	66.6	67.3	69.0	69.1
		66.6													
$\text{CH}_2\text{-CH-CH}_2$	62.1	63.6	63.1	64.1	61.4	61.4	62.3	63.8	61.3	62.1	62.5	64.7	63.6	61.3	61.5
C=O	173.3	172.0	173.2	173.7	173.3	173.3	172.1	173.9	173.3	173.3	171.4	172.9	173.1	173.1	73.4
	172.8		172.4	173.2	172.5	172.5		173.3	172.5	172.8				172.3	172.5
CH=CH	130.0	129.2	129.5	130.0	129.1	129.1	129.3	129.9	129.1	130.0	129.2	128.8	129.9	128.9	129.0
	129.7			128.7				127.8		129.7			129.0		
CH <sub>3</sub>	14.1	14.2	15.1	14.8	15.1	15.1	14.3	15.2	14.9	14.0	14.2	15.0	15.5	15.0	15.1
			14.3	14.4	13.9	13.9		14.6	13.9			14.3	14.5	13.8	13.9
				13.9				14.1							

<sup>a</sup>See Table 1 for abbreviations.

**FIG. 1.**  $^{13}\text{C}$  cross-polarization and magic-angle spinning nuclear magnetic resonance (CP/MAS-NMR) spectra of glycerol regions obtained for the five polymorphic forms of 1,3-distearoyl-2-oleoyl glycerol. The peaks at 73–76 ppm are due to the spinning side bands (SSB).**FIG. 2.**  $^{13}\text{C}$  CP/MAS-NMR spectra of carbonyl regions, obtained for the five polymorphic forms of 1,3-distearoyl-2-oleoyl glycerol. See Figure 1 for abbreviation.

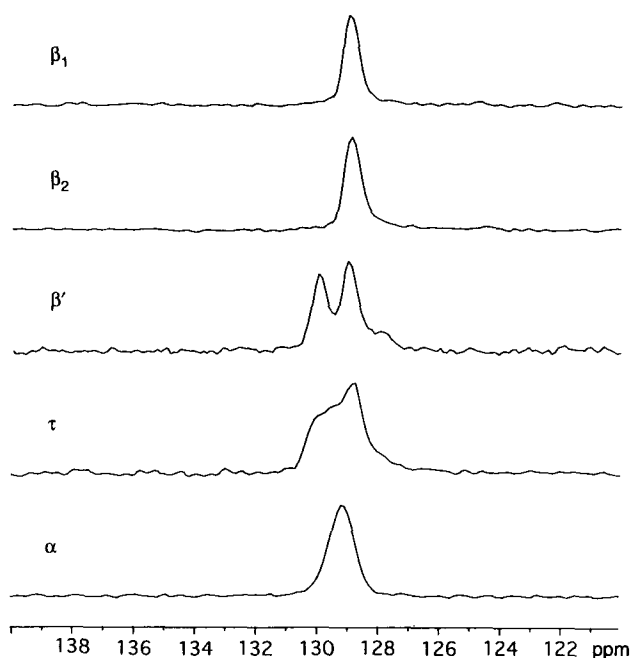


FIG. 3.  $^{13}\text{C}$  CP/MAS-NMR spectra of olefin regions, obtained for the five polymorphic forms of 1,3-distearoyl-2-oleoyl glycerol. See Figure 1 for abbreviation.

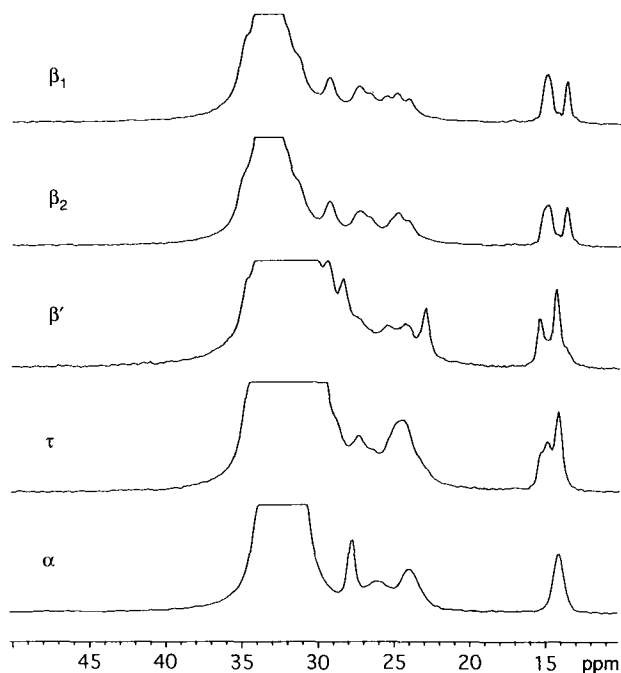


FIG. 4.  $^{13}\text{C}$  CP/MAS-NMR spectra of hydrocarbon regions, obtained for the five polymorphic forms of 1,3-distearoyl-2-oleoyl glycerol. See Figure 1 for abbreviation.

cates the existence of some distinction of different structures among the three carbonyl carbons. In the  $\beta_2$  and  $\beta_1$  form, two clearly separated peaks were noted at 172.3 and 173.1 for the

$\beta_2$  form and 172.5 and 173.4 ppm for the  $\beta_1$  form. The peak areas are approximately in the ratio of 2:1.

**Olefinic carbon.** Analysis of XRD and vibrational spectroscopy shows that olefinic conformations of *cis*-monounsaturated fatty acids, such as oleic acid, are greatly changed in the polymorphic transitions (12–15). The conformational diversity in the *cis* double bond in oleoyl chain may affect the polymorphism of Sat-O-Sat TAG. In the  $\alpha$  form, a single peak was observed at 129.2 ppm, indicating that the olefinic carbons at the ends of the *cis* double bond are equivalent. However, a smeared peak is obtained in the  $\gamma$  form, indicating that the olefinic carbons are no longer equivalent. The peak separation is clearer in the phase transition from  $\gamma$  to  $\beta'$ , and there are two peaks at 129.0 and 129.9 ppm, respectively. Thus, the conformation is asymmetric with respect to the *cis* double bond. However, the spectra of the olefinic carbons in the  $\beta_2$  and  $\beta_1$  forms appear as single resonances again, which implies similar environments at each end of the *cis* double bond.

**Methyl and Methylene carbons.** The terminal methyl carbons of the  $\alpha$  polymorphic form of SOS exhibit a single resonance peak at 14.2 ppm. Thus, the methyl end packings of stearoyl and oleoyl chains in a molecule are identical. In the  $\gamma$  and  $\beta'$  forms, two major peaks are observed for the methyl carbons with a ratio of 2:1. The peak at 15.5 ppm in the spectrum of the  $\gamma$  form suggests the presence of some  $\beta'$  crystals. The methyl carbons of  $\beta_2$  and  $\beta_1$  appear as two peaks. There is no difference between the spectra of the  $\beta_2$  and  $\beta_1$  forms in methyl carbons.

Spectral differences are also observed for the main methylene carbons. Especially around 24–26 ppm, the resonances of the  $\beta_1$  form differ from those of  $\beta_2$ . Due to the overlap of each carbon spectrum, most of the methylene carbons could not be assigned.

**POP and POS polymorphs.** The occurrence of polymorphic forms in POP and SOS is similar, except for the behavior of the metastable  $\beta'$  form (2). POS exhibits only  $\alpha$ ,  $\beta'$ , and  $\beta$  forms (4). Correspondingly,  $^{13}\text{C}$  NMR spectra of the polymorphic forms of POP and POS are mostly identical to those of SOS for the  $\alpha$ ,  $\beta_2$  and  $\beta_1$  forms. However, some spectral differences are observed in the glycerol and methyl regions of the  $\gamma$  and  $\beta'$  forms of POP and the  $\beta'$  form of POS. The glycerol carbons of the  $\gamma$  form of POP give four resonances at 59.6, 63.1, 66.6, and 67.3 ppm (Fig. 5). Hence, the glycerol conformation of POP differs from that of SOS. In addition, three resonance peaks were observed for the terminal methyl carbons of  $\beta'$  in POP and POS (Fig. 6). This shows that the carbons at the 1- and 3-position in the methyl region are not equivalent. Other spectra obtained from the polymorphic forms,  $\alpha$ ,  $\beta_2$ , and  $\beta_1$  of POP and  $\alpha$  and  $\beta$  of POS are equal to those of SOS.

## DISCUSSION

**Chemical shift of methylene carbons and crystal structure.** Recent progress in NMR spectroscopy has made it possible to discuss the crystal structure of molecules that contain hy-

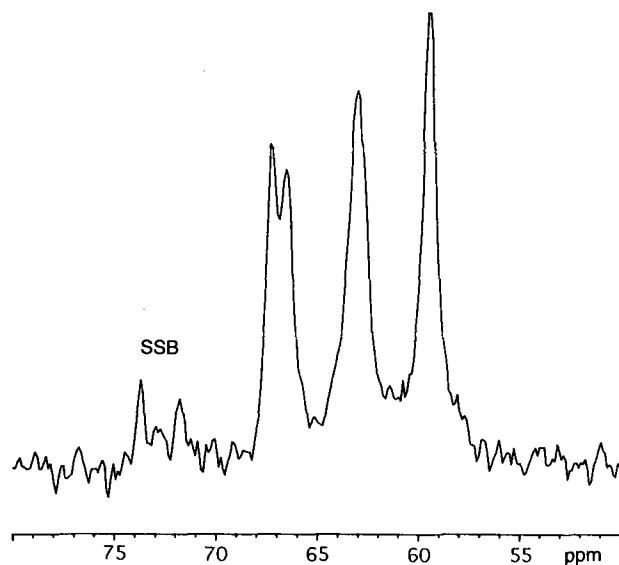


FIG. 5.  $^{13}\text{C}$  CP/MAS-NMR spectra of glycerol region, obtained for the  $\gamma$  form of 1,3-dipalmitoyl-2-oleoyl glycerol. The peaks at 71–74 ppm are due to the spinning side bands (SSB). See Figure 1 for abbreviation.

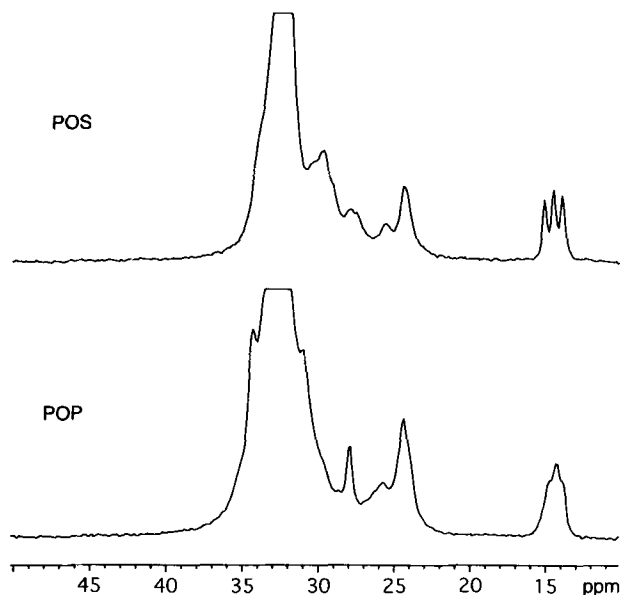


FIG. 6.  $^{13}\text{C}$  CP/MAS-NMR spectra of hydrocarbon regions, obtained for the  $\beta'$  forms of 1,3-dipalmitoyl-2-oleoyl glycerol (POP) and 1,3-*rac*-palmitoyl-stearoyl-2-oleoyl glycerol (POS). See Figures 1 and 5 for abbreviations.

drocarbon chains on the basis of the chemical shifts of the *trans* zigzag chains, as seen for *n*-paraffin and polyethylene (16,17). The chemical shifts of the *trans* zigzag carbons of orthorhombic, triclinic, and monoclinic structures are around 33, 34, and 35 ppm, respectively, (Spectra were referenced to the residual signal from the carbonyl carbon of glycine at 176.45 ppm relative to a TMS standard.).

The  $^{13}\text{C}$  chemical shifts of the main methylene carbons and the structures proposed for each of the polymorphic forms of POP, POS and SOS are summarized in Table 4. The structures

TABLE 4  
 $^{13}\text{C}$  Chemical Shifts of Main Methylene Carbons and Proposed Structures of POP, POS, and SOS Polymorph

Polymorph	Chemical shift (ppm)	Speculated structure	
POP	$\alpha$	32.7	Hexagonal
	$\gamma$	33.7	N.S. <sup>a</sup>
	$\beta'$	32.7	Orthorombic
	$\beta_2$	33.7	Triclinic
	$\beta_1$	33.7	Triclinic
POS	$\alpha$	32.8	Hexagonal
	$\beta'$	32.5	Orthorombic
	$\beta$	33.6	Triclinic
SOS	$\alpha$	32.6	Hexagonal
	$\gamma$	33.4	N.S.
	$\beta'$	32.2	Orthorombic
	$\beta_2$	33.6	Triclinic
	$\beta_1$	33.6	Triclinic

<sup>a</sup>Not specified. See Table 1 for abbreviations.

were determined by comparing the chemical shifts found in the present work with those previously found for similar compounds (16,17). The chemical shifts of the  $\alpha$  form of POP, POS, and SOS are in the middle of the chemical shift of orthorhombic and hexagonal structures. From the XRD and FT-IR analysis; however, it is recognized that the structure of the  $\alpha$  form has a hexagonal packing (2,6). This ambiguity may be due to the complexity of oleoyl chains. The chemical shifts of main methylene carbons for the  $\beta$  polymorphic forms of three TAG are in agreement with the values of triclinic structure of polyethylene.

FT-IR analyses concerning the subcell structures of oleoyl chains of  $\beta_2$  and  $\beta_1$  assumed  $\text{O}'_{//}$  and  $\text{T}_{//}$  respectively, suggesting that the structural difference between  $\beta_2$  and  $\beta_1$  forms of POP and SOS may appear in the oleoyl chain (6). In the present study, no chemical shift differences in the regions of polymethylene chains were observed in the  $\beta_2$  and  $\beta_1$  of POP and SOS. This may still leave an open question as to the difference in the chemical shift between the  $\text{T}_{//}$  and  $\text{O}'_{//}$  subcell structure, the latter being observed in low-temperature forms of *cis* monounsaturated fatty acids (12).

The chemical shifts of the  $\beta'$  forms of the three TAG are close to those of orthorhombic crystals of polyethylene. This is also consistent with previous XRD and FT-IR analysis (2,6). The structures of the  $\gamma$  forms of POP and SOS are not specified; this may be due to the structural complexity of the  $\gamma$  form.

**Total polymorphic structure.** The spectra of the  $\alpha$  forms of POP, POS, and SOS are almost identical. From the appearance of two broad peaks and the integral ratio of 2:1 (Fig. 1), the glycerol conformation of the  $\alpha$  form is similar to that in the liquid state. The carbonyl, olefinic, and methyl carbon resonances, respectively, appear as single broad peaks, suggesting that the saturated and oleoyl chains formed disordered packing in a hexagonal-like structure. Similar tendencies were observed in tripalmitin (PPP) (9), which is consistent with the proposed molecular organization of this form (10,11).

The glycerol conformations in the  $\gamma$  forms of POP and SOS exhibited complicated behavior because the carbon atoms are not magnetically equivalent. This complexity may be related to chain sorting, which gives rise to separation of the chains of saturated and oleoyl chains to form the triple chainlength structure (2). Olefinic conformations of  $\gamma$  are also different from those of  $\alpha$ . The peak separation of the olefinic carbons implies different conformations at each end of the *cis* double bond. However, methyl end-packing of the  $\gamma$  form may still be equivalent in the saturated acyl chains but not in the oleoyl chains.

The methyl carbon regions in the spectra of  $\beta'$  forms are different in POP, POS, and SOS. The methyl carbons of saturated acyl chains are equivalent in SOS but not in POP and POS. This is related to differences in the chain inclination in the  $\beta'$  form. From analysis of the X-ray powder diffraction, the saturated acyl chains of  $\beta'$  are inclined at  $72^\circ$  to the basal plane (2). Subtle chainlength differences in the saturated moieties may affect the angle of inclination.

It is confirmed, from the appearance of split peaks, that olefinic carbons of  $\beta'$  are not equivalent. These peak separations in the olefinic carbons are also observed in the  $\alpha$  form of oleic acid, which exhibits partially disordered packing in the *cis* double bond to methyl region (Sugimoto, R., unpublished data). Therefore, the partial aliphatic chains from the *cis* double bond to the methyl end group in  $\beta'$  may be in a conformationally disordered state.

In the  $\beta_2$  forms of POP and SOS, the saturated acyl chains have almost identical conformations because two peaks are observed with integrals in a 2:1 ratio for the carbonyl and methyl carbons. Single resonance peaks are obtained for the olefinic carbons, indicating that the oleoyl chains in the  $\beta_2$  form have a symmetric conformation around the *cis* double bond.

In our previous studies, thermal and structural differences between  $\beta_2$  and  $\beta_1$  of POP and SOS were reflected in the melting points, XRD short- and long-spacing spectra (2), crystal morphologies (3), crystal densities (5), and FT-IR absorbance spectra (6). It has been thought that these differences may be due to conformational changes from  $O'_{//}$  to  $T_{//}$  in the oleoyl chain. In the present study, there are no large differences in the glycerol, carbonyl, olefinic, and methyl regions between  $\beta_2$  and  $\beta_1$ . Small differences are, however, observed in the methylene region. Namely, the peak at 25.9 ppm appears only in the  $\beta_1$  form. A complete assignment of the peaks in this region is difficult due to the spectral overlap. However, it is likely that some structural changes in oleoyl chains occur during the  $\beta_2 \rightarrow \beta_1$  transition.

The results obtained in the present study are in good agreement with previous results. This CP/MAS technique is a powerful method for examining the structure of metastable and stable forms, and it provides complementary information to that obtained from FT-IR analysis.

## ACKNOWLEDGMENTS

We are grateful to Dr. K. Hayami and Dr. W.S. Price, National Institute of Materials and Chemical Research, for valuable advice.

## REFERENCES

1. Sonntag, N.O.V., Composition and Characteristics of Individual Fats and Oils, in *Bailey's Industrial Oil and Fats Products*, Vol. 1, 4th edn., edited by D. Swern, John Wiley & Sons, New York, 1979, pp. 322–332.
2. Sato, K., T. Arishima, Z.H. Wang, K. Ojima, N. Sagi, and H. Mori, Polymorphism of POP and SOS., I. Occurrence and Polymorphic Transformation., *J. Am. Oil Chem. Soc.* 66:664–674 (1989).
3. Arishima, T., and K. Sato, Polymorphism of POP and SOS. III. Solvent Crystallization of  $\beta_2$  and  $\beta_1$  Polymorphs, *Ibid.* 66:1614–1617 (1989).
4. Arishima, T., N. Sagi, H. Mori, and K. Sato, Polymorphism of POS. I. Occurrence and Polymorphic Transformation, *Ibid.* 68:710–715 (1991).
5. Arishima, T., N. Sagi, H. Mori, and K. Sato, Density Measurement of the Polymorphic Forms of POP, POS, and SOS, *J. Jpn. Oil Chem. Soc.* 44:431–437 (1995).
6. Yano, J., S. Ueno, K. Sato, T. Arishima, N. Sagi, F. Kaneko, and M. Kobayashi, FT-IR Study of Polymorphic Transformations in SOS, POP and POS, *J. Phys. Chem.* 97:12967–12973 (1993).
7. Schaefer, J., E.O. Stejskal, and R. Buchdahl, High-Resolution  $^{13}\text{C}$  Nuclear Magnetic Resonance Study of Some Solid Glassy Polymers, *Macromolecules* 8:291–296 (1975).
8. Saito, H., Conformation-Dependent  $^{13}\text{C}$  Chemical Shifts: A New Means of Conformational Characterization as Obtained by High-Resolution Solid-State  $^{13}\text{C}$  NMR, *Magn. Reson. Chem.* 24:835–852 (1986).
9. Bociek, S.M., S. Ablett, and I.T. Norton, A  $^{13}\text{C}$ -NMR Study of the Crystal Polymorphism and Internal Mobilities of the Triglycerides, Tripalmitin and Tristearin, *J. Am. Oil Chem. Soc.* 62:1261–1266 (1985).
10. Hagemann, J.W., and J.A. Rothfus, Computer Modeling of Theoretical Structures of Monoacid Triglyceride  $\alpha$ -Forms in Various Subcell Arrangements, *Ibid.* 60:1308–1314 (1983).
11. Eads, T.M., A.E. Blaurock, R.G. Bryant, D.J. Roy, and W.R. Croasman, Molecular Motion and Transitions in Solid Tripalmitin Measured by Deuterium Nuclear Magnetic Resonance, *Ibid.* 69:1057–1068 (1992).
12. Kobayashi, M., F. Kaneko, K. Sato, and M. Suzuki, Vibrational Spectroscopic Study on Polymorphism and Order-Disorder Phase Transition in Oleic Acid, *J. Phys. Chem.* 90:6371–6378 (1986).
13. Kaneko, F., M. Kobayashi, Y. Kitagawa, Y. Matsuura, K. Sato, and M. Suzuki, Structure of the Low-Melting Phase of Petroselinic Acid, *Acta Crystallogr.* C48:1054–1057 (1992).
14. Kaneko, F., M. Kobayashi, Y. Kitagawa, Y. Matsuura, K. Sato, and M. Suzuki, Structure of the High-Melting Phase of Petroselinic Acid, *Ibid.* C48:1057–1060 (1992).
15. Kaneko, F., M. Kobayashi, Y. Kitagawa, Y. Matsuura, K. Sato, and M. Suzuki, Structure of the  $\gamma$  Phase of Erucic Acid, *Ibid.* C48:1060–1063 (1992).
16. Sorita, T., T. Yamanobe, T. Komoto, I. Ando, H. Sato, K. Deguchi, and M. Imanari,  $^{13}\text{C}$  NMR Chemical Shifts and Crystal Structures of Saturated Hydrocarbons, *Macromol. Chem., Rapid Commun.*, 5:657–659 (1984).
17. Yamanobe, T., T. Sorita, T. Komoto, and I. Ando,  $^{13}\text{C}$  Chemical Shift and Crystal Structure of Paraffins and Polyethylene as Studied by Solid State NMR, *J. Mol. Struct.* 131:267–275 (1985).

[Received July 26, 1995; accepted May 6, 1996]